High-Stability Semiquinone Intermediate in Nitrate Reductase A (NarGHI) from *Escherichia coli* Is Located in a Quinol Oxidation Site Close to Heme b_D[†]

Pascal Lanciano,[‡] Axel Magalon,[§] Patrick Bertrand,[‡] Bruno Guigliarelli,[‡] and Stéphane Grimaldi*[,‡]

Unité de Bioénergétique et Ingénierie des Protéines (UPR9036), and Laboratoire de Chimie Bactérienne (UPR9043), Institut de Biologie Structurale et de Microbiologie, CNRS and Université d'Aix-Marseille, 31 Chemin Joseph Aiguier, 13402 Marseille Cedex 20, France

Received January 15, 2007; Revised Manuscript Received February 28, 2007

ABSTRACT: Quinol/nitrate oxidoreductase (NarGHI) is the first enzyme involved in respiratory denitrification in prokaryotes. Although this complex in *E. coli* is known to operate with both ubi and menaquinones, the location and the number of quinol binding sites remain elusive. NarGHI strongly stabilizes a semiquinone radical located within the dihemic anchor subunit NarI. To identify its location and function, we used a combination of mutagenesis, kinetics, EPR, and ENDOR spectroscopies. For the $NarGHI_{H66Y}$ and $NarGHI_{H187Y}$ mutants lacking the distal heme b_D, no EPR signal of the semiquinone was observed. In contrast, a semiquinone was detected in the $NarGHI_{H56Y}$ mutant lacking the proximal heme b_P. Its thermodynamic properties and spectroscopic characteristics, as revealed by Q-band EPR and ENDOR spectroscopies, are identical to those observed in the native enzyme. The substitution by Ala of the Lys86 residue close to heme b_D, which was previously proposed to be in a quinol oxidation site of NarGHI (Q_D), also leads to the loss of the EPR signal of the semiquinone, although both hemes are present. Enzymatic assays carried out on the $NarGHI_{K86A}$ mutant reveal that the substitution dramatically reduces the rate of oxidation of both mena and ubiquinol analogues. These observations demonstrate that the semiquinone observed in NarI is strongly associated with heme b_D and that Lys86 is required for its stabilization. Overall, our results indicate that the semiquinone is located within the quinol oxidation site Q_D. Details of the possible binding motif of the semiquinone and mechanistic implications are discussed.

In anaerobiosis and in the presence of nitrate, *Escherichia coli* induces the production of two respiratory enzymes: formate dehydrogenase-*N* and dissimilatory nitrate reductase (NarGHI[1]). They cooperate in generating a proton motive force across the cytoplasmic membrane through the redox loop mechanism by coupling formate oxidation and nitrate reduction thanks to the lipid mobile electron/proton carrier mena or ubiquinol (*1*). The heterotrimeric NarGHI complex is composed of (i) a catalytic subunit NarG containing a MobisMGD cofactor and a [4Fe-4S] cluster, (ii) an electron-transfer subunit NarH carrying four FeS clusters, and (iii) a membrane-anchor subunit NarI containing two *b*-type hemes termed b_D and b_P to indicate their distal and proximal positions, respectively, with regard to the catalytic site (*2*−*4*).

We have recently characterized the thermodynamic and EPR spectroscopic properties of a semiquinone in membrane samples of overexpressed wild-type NarGHI (Figure 1B) (*5*). Using continuous wave (cw) ENDOR spectroscopy, we have unequivocally shown that this species is stabilized in a Q-site located within the membrane subunit NarI. Moreover, the semiquinone EPR signal disappears upon the addition of an excess of the menaquinone analogue 2-*n*-nonyl-4-hydroxyquinoline-*N*-oxide (NQNO). Remarkably, the semiquinone stability constant found in NarGHI is the largest measured so far in respiratory complexes stabilizing the semiquinone species. Stabilization of a semiquinone species in the quinol oxidation site of NarGHI could, in principle, occur during enzyme turnover because this Q site couples quinol oxidation (a two-electron process) to the reduction of hemes (a one-electron process) in two sequential one-electron steps. Alternatively, the radical species could arise from a nondissociable quinone bound within NarI. In this case, the quinone could act as a redox cofactor similar to Q_H in bo_3 quinol oxidase from *E. coli* (*6*), Q_A in bacterial photosynthetic reaction centers (*7*), or phylloquinones A_1 in photosystem I (*8*). Altogether, this raises the question of the function of this radical species in the catalytic mechanism and of its precise location within NarI.

In the available crystal structure of NarGHI, no bound quinone could be resolved (*2*). Nevertheless, a crystal structure of the enzyme carrying a single point mutation C26A in NarH and in which a potent quinol binding inhibitor pentachlorophenol (PCP) is present, has been solved (*9*). It shows that PCP binds on the periplasmic side of the enzyme,

[†] This work was supported by the CNRS, the Université de Provence, and the Agence Nationale de la Recherche (project PCV/ERMoE). P.L. was supported by a MRT fellowship.

* Corresponding author. Phone: (+00 33) 491164557. Fax: (+00 33) 491164578. E-mail: grimaldi@ibsm.cnrs-mrs.fr.

[‡] Unité de Bioénergétique et Ingénierie des Protéines (UPR9036).

[§] Laboratoire de Chimie Bactérienne (UPR9043).

[1] Abbreviations: cw, continuous wave; ENDOR, electron nuclear double resonance spectroscopy; EPR, electron paramagnetic resonance spectroscopy; HQNO, 2-heptyl-4-hydroxyquinoline-*N*-oxide; NarGHI, *E. coli* dissimilatory membrane bound quinol/nitrate oxidoreductase A; NQNO, 2-nonyl-4-hydroxyquinoline-*N*-oxide; PCP, pentachlorophenol; Q site, quinone binding site; SQ, semiquinone radical.

10.1021/bi700074y CCC: $37.00
Published on Web 04/18/2007

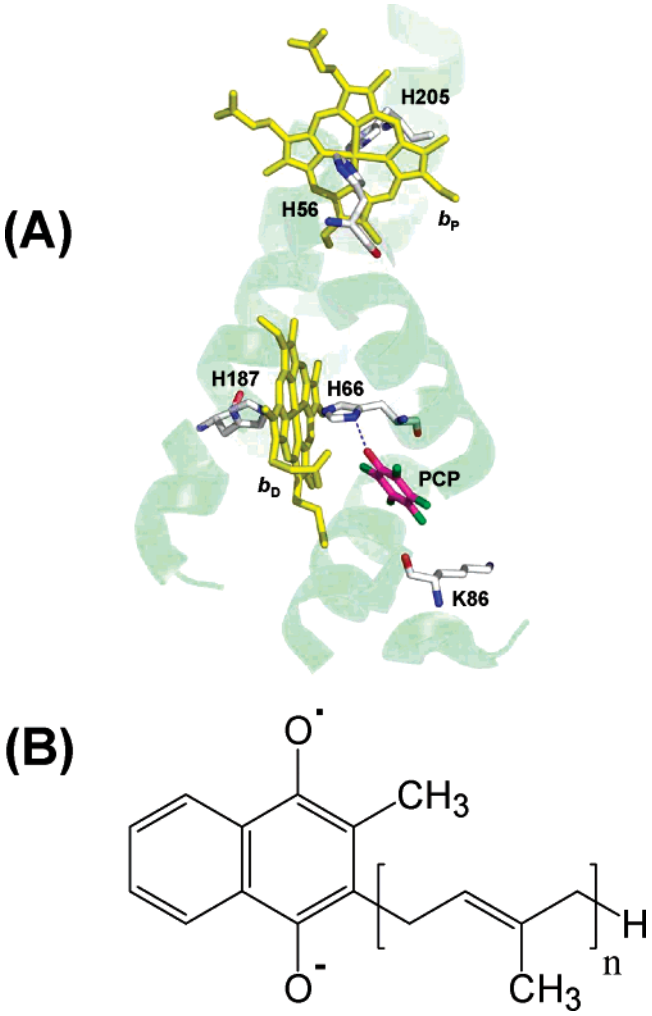

FIGURE 1: (A) Location of the aminoacids in the NarI subunit that were mutated and investigated in this work. The position of the inhibitor PCP is also shown (pdb entry 1Y4Z). (B) Molecular structure of the menasemiquinone anion.

in close proximity to heme b_D. Indeed, the inhibitor makes a hydrogen bond with the His66 residue, an axial ligand of heme b_D (Figure 1A). From mutagenesis experiments and molecular modeling studies of a quinol molecule in the PCP binding site, it has been proposed that the Lys86 residue located in the PCP binding site may act as a second hydrogen bond donor for a putative quinol molecule (*9*). The presence of a second Q site in NarI has been proposed on the basis of kinetic data (*10*), which could be located in an elongated hydrophobic cavity exposing both hemes to the lipid bilayer (*2*). Steady-state kinetic studies have, moreover, suggested that ubi and menaquinol analogues may deliver their electrons at two different sites of the nitrate reductase (*11*, *12*).

To provide a foundation for understanding the mechanism of quinol utilization by the respiratory nitrate reductase complex, it is first necessary to define the location of the observed semiquinone radical species. Here, we have extended our initial studies by probing the effect of the selective removal of one of the hemes on the spectroscopic and thermodynamic properties of the semiquinone. The effect of the substitution of Lys86 by Ala was also investigated. Our results show unambiguously that the semiquinone is strongly associated with heme b_D and that Lys86 is required for the stabilization of the semiquinone in the enzyme. This residue appears to be essential for oxidizing menaquinol and ubiquinol analogues as well.

EXPERIMENTAL PROCEDURES

Bacterial Strain and Plasmids. E. coli nar-deficient strain, LCB3064 (*nar25(nar*GH*)*, *narZ::*Ω, Δ*nap*, *thi*-1, *leu*-6, *thr*-1, *rps*L175, *lac*Y, Kan^R, and Spc^R (Cole, J., School of Biosciences, University of Birmingham, U.K.)) was used as a host for the experiments described herein. NarGHI was expressed from plasmid pVA700 (Amp^r), which encodes the *narGHJI* operon under the control of the tac promoter (*13*). Other plasmids used in this work were pVA700-H66Y (*14*), pVA700-H187Y (*10*), pVA700-H56Y (this work), and pVA700-K86A (*9*), encoding $NarGHI_{H66Y}$, $NarGHI_{H187Y}$, $NarGHI_{H56Y}$, and $NarGHI_{K86A}$, respectively.

Growth Conditions and Preparation of Membrane Fractions. Cells were grown semianaerobically in a 2.5 L Erlenmeyer flask containing Terrific Broth medium at 37 °C (*15*). Enzyme overexpression was obtained by the addition of 0.2 mM isopropyl 1-thio-β-D-galactopyranoside. When appropriate, ampicillin (100 μg mL^{-1}), spectinomycin (50 μg mL^{-1}), and kanamycin (50 μg mL^{-1}) were included in the growth medium. Cells were harvested and washed, and membranes were prepared by French press cell lysis and differential centrifugation (*16*). Enriched inner membrane vesicles were prepared from these crude membranes by sucrose step centrifugation (*17*). Membrane vesicles were suspended in 100 mM MOPS and 5 mM EDTA at pH 7.5 and stored at −80 °C until use.

Membrane preparations were assayed for protein concentration by the method of Lowry et al. (*18*). Immunological quantitation of NarGHI was achieved using rocket immunoelectrophoresis as described in ref 19 (*19*). The NarGHI concentration was estimated to be in the 40 to 120 μM range, depending on preparations.

Enzymatic Assays. Quinol/nitrate oxidoreductase activities were spectrophotometrically measured according to ref 20 (*20*) by the absorption changes caused by the oxidation of the ubiquinol analogues tetramethyl-*p*-benzoquinol (duroquinol, $E_0 = +35$ mV) and 2,3-dimethoxy-5-methyl-6-decyl-1,4-benzoquinol (decylubiquinol, $E_0 = +100$ mV), and the menaquinol analogues 2-methyl-1,4-naphtoquinol (menadiol, $E_0 = 0$ mV), 5-hydroxy-2-methyl-naphthalene-1,4-diol (plumbagin, $E_0 = -74$ mV), and 5-hydroxy-1,4-naphthoquinol (juglone $E_0 = +33$ mV) by nitrate. A 20 mM stock ethanolic solution of each quinone analogue was reduced by metallic zinc in acidified ethanol. Assays were initiated by the addition of nitrate (37 mM) to the anaerobic assay buffer containing the subcellular fractions and the electron donors (200 μM). The difference of millimolar extinction coefficients (redox) used for menadiol, duroquinol, decylubiquinol, juglone, and plumbagin are $\epsilon_{260} = 17.2$, $\epsilon_{260} = 21.3$, $\epsilon_{279} = 12.3$, $\epsilon_{245} = 12.6$, and $\epsilon_{255} = 15.8$, respectively.

Redox Titration Experiments. Redox titrations were performed anaerobically as described in ref 5 (*5*). Redox potentials were adjusted with small additions of 100 mM sodium dithionite and measured with a combined Pt−Ag/AgCl/KCl (3 M) microelectrode in the presence of the same mediators (each at 10 μM concentration) previously used for the titration of the wild-type enzyme (*5*). Stable potentials were achieved in a few minutes, and samples were anaero-

bically transferred into calibrated EPR tubes that were rapidly frozen. All quoted potentials are given with respect to the standard hydrogen electrode.

EPR and ENDOR Spectroscopies. EPR measurements were performed on a Bruker Elexsys E500 spectrometer. X-band EPR spectra were recorded using a standard rectangular Bruker cavity (ST 4102) fitted to an Oxford Instruments Helium flow cryostat (ESR900). Q-band EPR spectra were recorded using a standard Bruker resonator (ER 5106QT) equipped with an Oxford Instruments CF 935 cryostat. For *g*-value measurements, the microwave frequency was measured by using a Hewlett-Packard HP1552B frequency counter, and magnetic field values were corrected against a known *g* standard (weak pitch, $g = 2.0028 \pm 0.0001$). The simulation of powder spectra was carried out using a program described in ref 21 (*21*). The powder spectrum given by a disordered frozen solution is obtained by summation over approximately 1000 orientations uniformly distributed on a half sphere. In order to account for inhomogeneous broadening effects, the spectrum is then convoluted with an isotropic Gaussian line.

^{1}H ENDOR spectra were recorded using a Bruker DICE extension, a 250 W radio frequency amplifier from Amplifier Research and a Bruker EN 801 X-band cw ENDOR resonator. They are presented in the first-derivative mode. The radio frequency wave was modulated at 25 kHz with a modulation depth of 200 kHz. For isotropic ENDOR spectra of weakly coupled protons, each proton is expected to give rise to two lines that are symmetrically spaced with respect to the proton nuclear Larmor frequency ν_H and separated by the proton hyperfine coupling constant, *A*. The ENDOR frequencies, ν_{ENDOR}, are, therefore, given by $\nu^{\pm}_{ENDOR} = \nu_H \pm A/2$ (*22*).

RESULTS

Specific Loss of the Semiquinone Radical EPR Signal in the Absence of the Heme b_D. The use of optical and EPR spectroscopies, in combination with mutagenesis studies and redox potentiometry, has allowed for the determination of the coordination and redox properties of both hemes (*14*, *15*). These hemes display highly anisotropic low-spin EPR spectra in which only the absorption-like g_z feature is detectable. Heme b_D has a midpoint potential of $E_{m,7} = +20$ mV. It is located on the periplasmic side of NarI and is coordinated by His66 and His187 (Figure 1A). Heme b_P is located on the cytoplasmic side. It is coordinated by His56 and His205 and has a midpoint potential of $E_{m,7} = +125$ mV. The selective mutation of one of these histidines into tyrosine or arginine leads to the loss of the corresponding coordinated heme (*10*, *14*, *15*). Taking advantage of this property, we have examined the effect of the selective suppression of one of the hemes on the semiquinone EPR signal in membrane preparations of the NarGHI$_{H66Y}$, NarGHI$_{H187Y}$, and NarGHI$_{H56Y}$ mutants. The heme content of the mutants in fully oxidized membranes was first checked by EPR spectroscopy. The $g = 3.36$ signal due to heme b_D was not visible in the EPR spectra of the NarGHI$_{H66Y}$, as previously observed (*14*). The same result was obtained in the case of the NarGHI$_{H187Y}$ mutant. Likewise, the NarGHI$_{H56Y}$ mutant did not exhibit the $g = 3.76$ signal from heme b_P. In each mutant, the signal given by the remaining heme was identical to that found in the wild-type enzyme (data not shown).

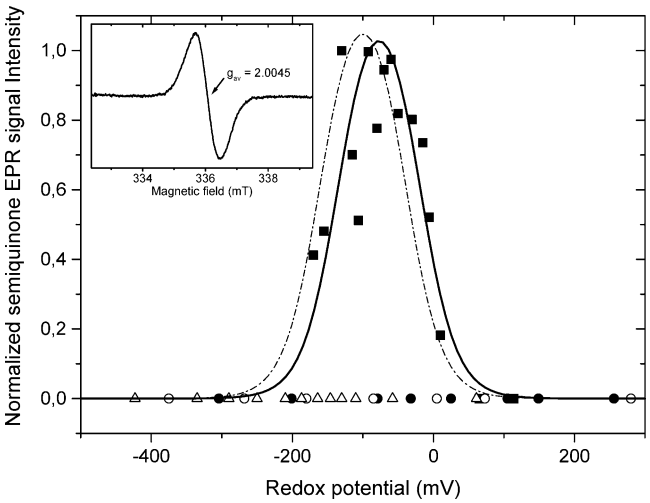

FIGURE 2: Potentiometric redox titration curves for the semiquinone in the NarGHI$_{H56Y}$ (the solid line displays the theoretical Nernst fit of the data points shown as filled squares), NarGHI$_{H66Y}$ (●), NarGHI$_{H187Y}$ (○), and NarGHI$_{K86A}$ (△) mutated nitrate reductase A from *E. coli* at pH 7.5 in membrane fractions. The peak-to-peak amplitude measured at $g \approx 2$ is plotted as a function of the ambient potential. The fit of the titration curve of the radical in wild-type NarGHI is recalled as dotted lines for comparison (*5*). Semiquinone EPR spectra were recorded under the following conditions: temperature, 80 K; microwave power, 10 μW; modulation amplitude, 0.3 mT; modulation frequency, 100 kHz; and microwave frequency, 9.425 GHz. The insert shows the EPR spectrum of the SQ in the NarGHI$_{H56Y}$ membrane redox poised at −120 mV and recorded under the same conditions as those described above except that the microwave power was set to 0.1 mW.

Potentiometric titrations of the three mutants were performed in the redox potential range −400 to +300 mV, and the redox poised samples were examined by EPR spectroscopy at 80 K to detect semiquinone signals. The results are shown in Figure 2, where the semiquinone titration curve of the wild-type enzyme is recalled as a dotted line (*5*). In the case of the NarGHI$_{H66Y}$ and NarGHI$_{H187Y}$ mutants, no significant radical signal was detected, indicating either the nonbinding of the quinone in these mutants or a strong destabilization of the bound semiquinone radical rendering it EPR-undetectable (see Discussion). In contrast, the NarGHI$_{H56Y}$ mutant lacking heme b_P exhibited a radical-type signal with a shape and average *g* value similar to those of the semiquinone signal characterized in the wild-type enzyme, that is, $g_{av} = 2.0045$ and a line width of 0.85 mT (Figure 2, inset). This radical titrates according to a bell-shaped curve, which is slightly shifted toward higher redox potentials by comparison with that observed for the SQ in the wild-type enzyme. A curve-fitting computer analysis yields $E_1 = -20 \pm 10$ mV and $E_2 = -135 \pm 10$ mV, where E_1 and E_2 are the midpoint potentials of the Q/SQ and SQ/QH$_2$ couples, respectively. From these values, a stability constant K_s of ∼80 can be calculated, which is similar to the K_s of ∼70 measured in the wild-type enzyme (*5*). The semiquinone concentration was determined by a double integration of its spectrum recorded under nonsaturating conditions. By using the [3Fe-4S]$^{1+}$ clusters of a fully oxidized sample as an internal standard, the maximal concentration of the radical species was estimated to be 0.43 ± 0.05 SQ/[3Fe-4S] cluster.

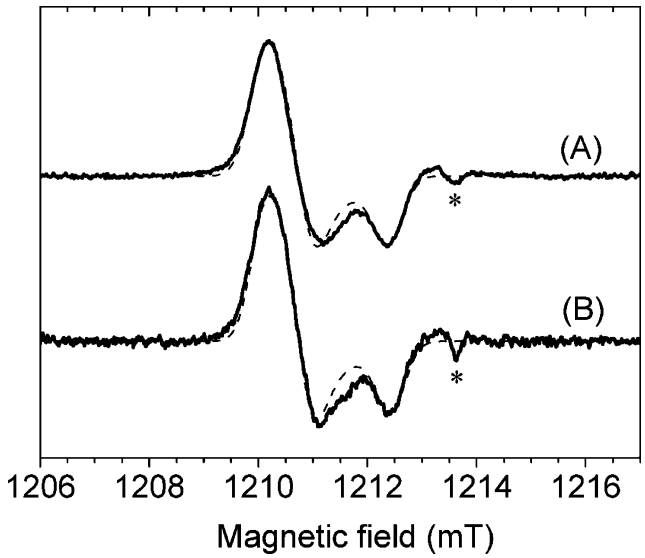

FIGURE 3: Q-band EPR spectra of the semiquinone in membrane samples of overexpressed NarGHI poised at −110 mV. (A) Wild-type enzyme. (B) NarGHI$_{H56Y}$. Experimental conditions: temperature, 80 K; microwave power, 0.5 μW; microwave frequency, 33.9 GHz; modulation amplitude, 0.5 mT; and modulation frequency, 100 kHz. Numerical simulations of both spectra are shown as dotted lines. They have been obtained using the same set of parameters, that is, $g_x = 2.0061$, $g_y = 2.0051$, $g_z = 2.0023$ ($\pm$0.0001), and an isotropic Gaussian line width of 0.385 mT. The signals indicated by asterisks are artefacts due to impurities in the cavity.

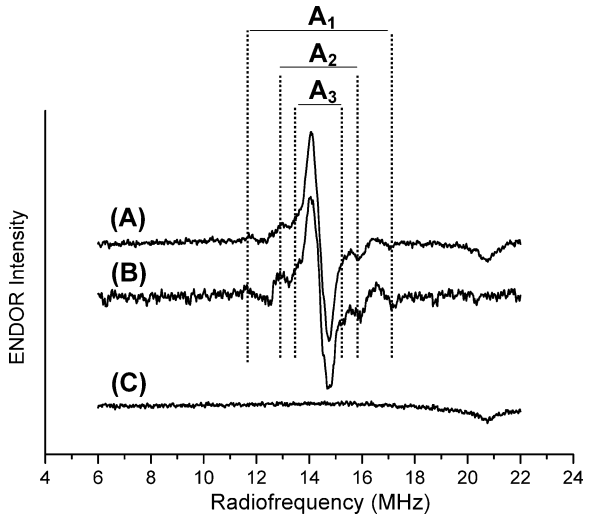

FIGURE 4: ENDOR spectra of membrane samples of the NarGHI$_{H56Y}$ mutant (A, C) and the wild-type enzyme (B). The static magnetic field was set at the maximum absorption of the semiquinone (A and B) and out of the EPR resonance line of the radical (C) 336 mT. Other experimental conditions: temperature, 80 K; microwave frequency, 9.477 GHz; microwave power, 5 mW; radiofrequency power, 110 W; modulation depth, 200 kHz; modulation frequency, 25 kHz; RF sweep width, 16 MHz; time constant and conversion time, 20.48 ms; gain, 60 dB; number of accumulations, 2500 (A), 1680 (B), and 710 (C); and redox potential, −116 mV (A and C) and −90 mV (B).

Q-Band EPR and ENDOR Characterizations of the Radical in the Mutant NarGHI$_{H56Y}$. To compare more precisely the spectroscopic characteristics of the radical species observed in the mutant NarGHI$_{H56Y}$ and in the wild-type enzyme, higher resolution techniques such as Q-band EPR and ENDOR spectroscopies were used. The Q-band EPR spectra displayed by the two forms of the enzyme are shown in Figure 3. They exhibit the same characteristic axial line shape, and the *g* values deduced from the numerical simulations are identical (Figure 3). Thus, the loss of heme b_P does not affect the semiquinone EPR signal.

A cw ENDOR study of the radical in the mutant NarGHI$_{H56Y}$ was carried out to probe its electronic structure. The spectrum recorded with the static magnetic field set at the center of the radical EPR spectrum is shown in Figure 4A. It displays proton ENDOR line shapes and hyperfine coupling values similar to those detected in the spectrum of the wild-type enzyme recorded under the same experimental conditions (Figure 4B). Indeed, three pairs of ENDOR signals symmetrically positioned with respect to the free proton Larmor frequency ($\nu_H \sim$14.4 MHz) and corresponding to hyperfine couplings equal to $A_1 = 5.7$ MHz, $A_2 = 3.3$ MHz, and $A_3 = 1.8$ MHz can be observed in both the mutant and the wild-type enzyme. These resonances were not observed when the static magnetic field was set outside the semiquinone EPR spectrum (Figure 4C). These hyperfine couplings are similar to those measured for other protein-bound SQ radicals, which were assigned to (i) nonexchangeable (for example, methyl or methylene) protons of the quinone, (ii) exchangeable protons forming, for example, hydrogen bonds with the quinone carbonyl oxygens, or (iii) protons of aminoacids in the vicinity of the semiquinone (*23*−*29*). The detailed analysis of the ENDOR spectra and the attribution of the detected ENDOR features to specific protons are in progress. The available data show that the magnitude of the proton hyperfine couplings is strongly dependent on the electronic structure of the semiquinone and its close environment. Thus, it is concluded that the semiquinone observed in the mutant NarGHI$_{H56Y}$ has the same electronic structure as that found in the wild-type enzyme and that they bind within the same site. Therefore, the loss of heme b_P does not affect the binding of the SQ.

Substitution of the K86 Residue Results in the Loss of the Semiquinone EPR Signal. In the previous section, we have shown that heme b_D is required for stabilizing the semiquinone. Because a molecular modeling study has suggested that Lys86 located close to heme b_D may act as a hydrogen bond donor to a quinone, we have studied the effect of the K86A mutation on the stabilization of the semiquinone radical. The potentiometric titration of the mutant NarGHI$_{K86A}$ was performed by using experimental conditions and a redox potential range the same as those for the other mutants. At first, the g_z component of the rhombic EPR signal of heme b_D was measured at 3.28, which is slightly shifted with respect to the value of 3.36 measured in the wild-type enzyme (Figure 5, insert). The normalized intensities of hemes b_D and b_P low-field EPR signals are plotted versus the ambient redox potential in Figure 5. Heme b_D titrates with an $E_{m,7.5}$ value of $+40 \pm 10$ mV, a value very similar to the previously reported $E_{m,7} = +20 \pm 10$ mV (*14*, *17*). In contrast, heme b_P ($g = 3.76$) titrates with an $E_{m,7.5}$ value of $+80 \pm 10$ mV, which differs more significantly from the value of $\pm$120 mV previously measured at pH 7 (*14*, *17*). Thus, it appears that the mutation K86A affects not only the spectroscopic properties of heme b_D but also the redox behavior of heme b_P. More significantly, no semiquinone EPR signal could be detected in NarGHI$_{K86A}$ membrane fractions (Figure 2), although heme b_D is present. Thus,

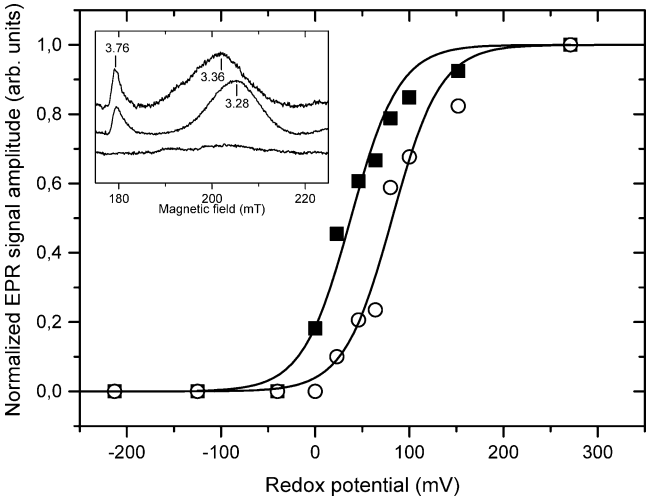

FIGURE 5: Redox titration of hemes b_D and b_P in the NarGHI$_{K86A}$ mutant. EPR signal amplitudes of hemes b_D ($g_z = 3.28$, ■) and b_P ($g_z = 3.76$, ○) were measured vs the ambient redox potential in the presence of mediators as described in Experimental Procedures. A third-order polynomial baseline correction was applied to the experimental spectrum in order to remove the background signal arising from free iron. Signal intensities were fitted to a Nernst plot, yielding an estimated $E_{m,7.5}$ of +40 mV and +75 mV for hemes b_D and b_P, respectively, with an estimated error of ±10 mV. EPR signal intensities are normalized with respect to the maximal EPR signal amplitude obtained for each heme. The insert shows the EPR spectrum of the low-spin heme of NarGHI (top) and NarGHI$_{K86A}$ (middle) in *E. coli* membranes. The spectrum at the bottom (in the insert) corresponds to the signal recorded in *E. coli* membranes devoided of NarGHI. Heme *g* values are indicated on the spectra. The EPR spectra were recorded under the following conditions: temperature, 12.5 K; microwave power, 20 mW at 9.4 GHz; modulation amplitude, 1 mT; modulation frequency, 100 kHz; and number of accumulations, 9.

Lys86 is required for stabilizing the semiquinone in the enzyme.

Enzymatic Assays of the Mutant NarGHI$_{K86A}$ in the Presence of Various Electron Donors. To investigate the role of Lys86 in the specific binding of menaquinones, ubiquinones, or both quinones, the quinol/nitrate oxidoreductase activity of the mutant NarGHI$_{K86A}$ was measured using different electron donors. At first, no activity was detected with the two ubiquinol analogues, duroquinol and decylubiquinol. In the same way, the activity using menaquinol analogues was strongly impaired. Indeed, in comparison with the wild-type enzyme, the activity value was found equal to 0%, 2%, and 14% with menadiol, juglone, and plumbagin, respectively. These results suggest that the Q_D site accommodates the two types of quinol in different ways.

DISCUSSION

We have previously characterized a highly stabilized semiquinone radical in NarGHI and have shown that it is located within the NarI subunit. In the present work, we have described the potentiometric and EPR spectroscopic study of several NarI mutants. A semiquinone signal was detected in the mutant NarGHI$_{H56Y}$, which lacks heme b_P. Its thermodynamic and EPR spectroscopic properties are very similar to those measured in the wild-type enzyme. Moreover, ENDOR spectroscopy experiments have shown that the hyperfine interactions of the radical are the same in the wild-type and in the mutant protein. This demonstrates that the radical is bound within the same site in the two forms of the enzyme and that its binding is not affected by the loss of heme b_P. This suggests that this site is remote from heme b_P.

The semiquinone EPR signature was lost in both NarGHI$_{H66Y}$ and NarGHI$_{H187Y}$ mutants, which lack heme b_D. This could result from the loss of protein-bound quinones as a consequence of the loss of heme b_D or from a destabilization of the radical state rendering it undetectable, although still bound to the enzyme. It was previously shown that the loss of heme b_D in the mutant NarGHI$_{H66Y}$ prevents high-affinity binding of the menaquinol-type inhibitor 2-heptyl-4-hydroxyquinoline-*N*-oxide (HQNO) (*17*) and increases the disorder of residues from the mutated Tyr66 to Thr72 (*9*). In this case, the mutation would be expected to also impair the binding of the natural quinone. From the available structural data, it has been proposed that a bound quinone may interact with the protein through hydrogen bonding with one of the propionate groups of heme b_D and with Nε-H66, as does the inhibitor PCP (Figure 1). In the mutant NarGHI$_{H187Y}$, heme b_D is lost, but His66 should be able to act as the hydrogen-bond donor to the quinone molecule. Our results suggest that the His66 residue is required for the stabilization of the SQ but that it cannot by itself maintain the semiquinone in a wild-type-like configuration when heme b_D is lost.

HQNO and PCP are known to act as inhibitors of the quinol/nitrate oxidoreductase activity of NarGHI (*9*, *17*, *30*). Upon binding, they also affect the spectroscopic properties of heme b_D. Additionally, fluorescence quench data have revealed a common binding site for PCP and HQNO (*9*). However, although the NarGHI$_{K86A}$ mutant attenuates the inhibitory effect of PCP compared to that measured in the wild-type enzyme, HQNO does not bind to this mutant (*9*). This can be explained by the fact that both H66 and K86 residues are required for correct binding of the HQNO molecule by providing hydrogen bonds to the inhibitor. We have recently observed that the SQ radical stabilized in the wild-type enzyme disappears upon the addition of an excess of NQNO, suggesting that the HQNO and the semiquinone binding sites overlap (*5*). Moreover, we have shown in the present work that the NarGHI$_{K86A}$ mutant is unable to stabilize the semiquinone radical, despite the presence of heme b_D and the His66 residue. This must be a direct consequence of the mutation because the structural characterization of this mutant indicates that the structure of NarGHI$_{K86A}$ is highly similar to that of the native enzyme (*9*). Thus, it is likely that the ability of quinones to bind to the mutated enzyme is severely impaired, explaining the absence of any detectable radical EPR signal in this mutant. The shift of the g_z component of heme b_D in this mutant is likely due to subtle changes of the local environment of the heme. The concomitant shift of the redox potential of heme b_P indicates that the tuning of the redox properties of both hemes in NarGHI is a complex mechanism that also involves long-range effects. Overall, our results show that Lys86 is a key residue involved in the stabilization of the radical. Taken together and given the location of Lys86 at the protein surface, at the entrance of the cavity housing the inhibitor PCP, all these data allow us to safely conclude that the semiquinone stabilized in the wild-type enzyme is located in the quinol oxidation site of NarGHI. Therefore, this radical

species is likely formed after the binding of a quinol molecule to the Q_D site and the transfer of one electron to heme b_D.

Although the available structural information for quinone reactive sites in respiratory and photosynthetic complexes shows very weak sequence and structural similarities (*31*), it can be noticed that a lysine residue appears to be essential for the quinol oxidase activity of the two other respiratory complexes known to stabilize an EPR-detectable semiquinone radical in their quinol oxidation site, namely, the *bd* quinol oxidase (*32*) and the FrdC-E29L mutant of *E. coli* fumarate reductase (FrdABCD) (*33*, *34*). FrdB-Lys228 located in the quinol oxidation site Q_P of the fumarate reductase from *E. coli* is found within hydrogen-bonding distance to menaquinone (*35*). Moreover, a recent site-directed mutagenesis study of the ubiquinol binding site in the *bd* quinol oxidase from *E. coli* shows that Lys252 is involved in quinol oxidation and may serve as the direct ligand and hydrogen bond acceptor for one ubiquinol carbonyl group (*36*). Interestingly, these lysine residues are strictly conserved among all fumarate reductases and *bd* quinol oxidases sequenced so far from various organisms. Lys86 is conserved as well in almost all sequenced nitrate reductases from gram negative bacteria. In addition, recent structural studies of the membrane-bound cytochrome *c* quinol dehydrogenase NrfH from *Desulfovibrio vulgaris* indicate that a highly conserved Lys residue (Lys 82) may be a hydogen bond donor for menaquinol in the proposed menaquinol oxidation site of this enzyme (*37*). The presence of a lysine residue in the quinol oxidation sites of NarGHI, fumarate reductase, and *bd* quinol oxidase could not only be important for the efficiency of the proton-shuttling mechanism during quinol oxidation as previously proposed for NarGHI (*9*) and fumarate reductase (*35*) but may also be an essential factor for tuning the thermodynamic stability of the semiquinone state in these enzymes. Remarkably, the stability constant of the SQ species differs in these three enzymes by several orders of magnitude, the largest being calculated for the semiquinone radical in NarGHI. The molecular factors responsible for these differences and the role of this stability during the enzymatic mechanism are not well understood. Interactions between quinone carbonyl oxygen atoms and H-bond-donating amino acid residues have been suggested to be an important factor in determining the properties of bound semiquinones. The present work supports the fact that His66 and Lys86 are interacting with the CO groups of the semiquinone radical, in agreement with the model proposed by Bertero et al. (*9*). Experiments using high-resolution EPR methods in combination with isotopically labeled quinones and solvents are currently being performed in our laboratory to study the detailed binding of the semiquinone radical in NarGHI and to assign the hyperfine couplings obtained from our ENDOR experiments to specific protons (*23*−*29*, *38*, *39*).

E. coli bd quinol oxidase, fumarate reductase, and NarGHI can use both mena and ubiquinols. The number of Q-sites in NarGHI and their specificity with respect to mena or ubiquinols, which have been investigated through various biochemical and biophysical approaches, are still a matter of debate (*2*, *5*, *9*−*12*, *40*). Using quinol/nitrate oxidoreductase activity measurements, we show that the substitution of Lys86 by Ala either prevents or drastically reduces the ability of the protein to oxidize both mena and ubiquinol analogues. Thus, although the structure of the $NarGHI_{K86A}$ mutant indicates that the quinol binding pocket is not significantly altered in the mutant form, enzymatic assays suggest that subtle changes in the Q_D site occur in the mutant, leading to a decrease of the protein binding affinity for all quinol analogues. Interestingly, *E. coli* cells expressing mutated $NarGHI_{K86A}$ enzymes can still grow under physiological conditions, that is, in anaerobic glycerol-nitrate minimal medium, albeit with a doubling time twice as low as that of the wild-type strain (data not shown). These results are in full agreement with our spectroscopic data and with their interpretation. However, they do not exclude the existence of a second auxiliary quinol oxidation site in the wild-type enzyme that may partially overcome the failure of the Q_D site. Overall, our enzymatic data indicate that Lys86 is essential for reactions with both types of quinol analogues and thus suggest that the oxidation of both mena and ubiquinols can occur at the Q_D site.

ACKNOWLEDGMENT

Rodrigo Arias-Cartin is gratefully acknowledged for the bacterial growth assays.

REFERENCES

1. Jormakka, M., Byrne, B., and Iwata, S. (2003) Protonmotive force generation by a redox loop mechanism, *FEBS Lett. 545*, 25−30.
2. Bertero, M. G., Rothery, R. A., Palak, M., Hou, C., Lim, D., Blasco, F., Weiner, J. H., and Strynadka, N. C. (2003) Insights into the respiratory electron transfer pathway from the structure of nitrate reductase A, *Nat. Struct. Biol. 10*, 681−687.
3. Blasco, F., Guigliarelli, B., Magalon, A., Asso, M., Giordano, G., and Rothery, R. A. (2001) The coordination and function of the redox centres of the membrane-bound nitrate reductases, *Cell. Mol. Life Sci. 58*, 179−193.
4. Rothery, R. A., Blasco, F., Magalon, A., and Weiner, J. H. (2001) The diheme cytochrome *b* subunit (NarI) of *Escherichia coli* nitrate reductase A (NarGHI): structure, function, and interaction with quinols, *J. Mol. Microbiol. Biotechnol. 3*, 273−283.
5. Grimaldi, S., Lanciano, P., Bertrand, P., Blasco, F., and Guigliarelli, B. (2005) Evidence for an EPR-detectable semiquinone intermediate stabilized in the membrane-bound subunit NarI of nitrate reductase A (NarGHI) from *Escherichia coli*, *Biochemistry 44*, 1300−1308.
6. Sato-Watanabe, M., Itoh, S., Mogi, T., Matsuura, K., Miyoshi, H., and Anraku, Y. (1995) Stabilization of a semiquinone radical at the high-affinity quinone-binding site (Q_H) of the *Escherichia coli bo*-type ubiquinol oxidase, *FEBS Lett. 374*, 265−269.
7. Lubitz, W., and Feher, G. (1999) The primary and secondary acceptors in bacterial photosynthesis. III. Characterization of the quinone radicals $Q_A^{-\bullet}$ and $Q_B^{-\bullet}$ by EPR and ENDOR, *Appl. Magn. Reson. 17*, 1−48.
8. Nelson, N., and Yocum, C. F. (2006) Structure and function of photosystems I and II, *Annu. Rev. Plant Biol. 57*, 521−565.
9. Bertero, M. G., Rothery, R. A., Boroumand, N., Palak, M., Blasco, F., Ginet, N., Weiner, J. H., and Strynadka, N. C. (2005) Structural and biochemical characterization of a quinol binding site of *Escherichia coli* nitrate reductase A, *J. Biol. Chem. 280*, 14836−14843.
10. Zhao, Z., Rothery, R. A., and Weiner, J. H. (2003) Effects of site-directed mutations on heme reduction in *Escherichia coli* nitrate reductase A by menaquinol: a stopped-flow study, *Biochemistry 42*, 14225−14233.
11. Giordani, R., Buc, J., Cornish-Bowden, A., and Cardenas, M. L. (1997) Kinetics of membrane-bound nitrate reductase A from *Escherichia coli* with analogues of physiological electron donors—different reaction sites for menadiol and duroquinol, *Eur. J. Biochem. 250*, 567−577.
12. Giordani, R., and Buc, J. (2004) Evidence for two different electron transfer pathways in the same enzyme, nitrate reductase A from *Escherichia coli*, *Eur. J. Biochem. 271*, 2400−2407.

13. Guigliarelli, B., Magalon, A., Asso, M., Bertrand, P., Frixon, C., Giordano, G., and Blasco, F. (1996) Complete coordination of the four Fe-S centers of the beta subunit from *Escherichia coli* nitrate reductase. Physiological, biochemical, and EPR characterization of site-directed mutants lacking the highest or lowest potential [4Fe-4S] clusters, *Biochemistry 35*, 4828−4836.
14. Magalon, A., Lemesle-Meunier, D., Rothery, R. A., Frixon, C., Weiner, J. H., and Blasco, F. (1997) Heme axial ligation by the highly conserved His residues in helix II of cytochrome *b* (NarI) of *Escherichia coli* nitrate reductase A, *J. Biol. Chem. 272*, 25652−25658.
15. Rothery, R. A., Blasco, F., and Weiner, J. H. (2001) Electron transfer from heme b_L to the [3Fe-4S] cluster of *Escherichia coli* nitrate reductase A (NarGHI), *Biochemistry 40*, 5260−5268.
16. Rothery, R. A., and Weiner, J. H. (1991) Alteration of the iron-sulfur cluster composition of *Escherichia coli* dimethyl sulfoxide reductase by site-directed mutagenesis, *Biochemistry 30*, 8296−8305.
17. Rothery, R. A., Blasco, F., Magalon, A., Asso, M., and Weiner, J. H. (1999) The hemes of *Escherichia coli* nitrate reductase A (NarGHI): potentiometric effects of inhibitor binding to narI, *Biochemistry 38*, 12747−12757.
18. Lowry, O. H., Rosebrough, N. J., Farr, A. L., and Randall, R. J. (1951) Protein measurement with the Folin phenol reagent, *J. Biol. Chem. 193*, 265−275.
19. Augier, V., Guigliarelli, B., Asso, M., Bertrand, P., Frixon, C., Giordano, G., Chippaux, M., and Blasco, F. (1993) Site-directed mutagenesis of conserved cysteine residues within the beta subunit of *Escherichia coli* nitrate reductase. Physiological, biochemical, and EPR characterization of the mutated enzymes, *Biochemistry 32*, 2013−2023.
20. Unden, G., and Kroger, A. (1986) Reconstitution of a functional electron-transfer chain from purified formate dehydrogenase and fumarate reductase complexes, *Methods Enzymol. 126*, 387−399.
21. Prisner, T., Lyubenova, S., Atabay, Y., MacMillan, F., Kroger, A., and Klimmek, O. (2003) Multifrequency cw-EPR investigation of the catalytic molybdenum cofactor of polysulfide reductase from *Wolinella succinogenes*, *J. Biol. Inorg. Chem. 8*, 419−426.
22. Kevan, L., and Kispert, L. D. (1976) *Electron Spin Double Resonance Spectroscopy*, Wiley-Interscience, New York.
23. Grimaldi, S., Ostermann, T., Weiden, N., Mogi, T., Miyoshi, H., Ludwig, B., Michel, H., Prisner, T. F., and MacMillan, F. (2003) Asymmetric binding of the high-affinity Q_H^- ubisemiquinone in quinol oxidase (*bo*$_3$) from *Escherichia coli* studied by multifrequency electron paramagnetic resonance spectroscopy, *Biochemistry 42*, 5632−5639.
24. Grimaldi, S., MacMillan, F., Ostermann, T., Ludwig, B., Michel, H., and Prisner, T. (2001) Q_H^- ubisemiquinone radical in the *bo*$_3$-type ubiquinol oxidase studied by pulsed electron paramagnetic resonance and hyperfine sublevel correlation spectroscopy, *Biochemistry 40*, 1037−1043.
25. Veselov, A. V., Osborne, J. P., Gennis, R. B., and Scholes, C. P. (2000) Q-band ENDOR (electron nuclear double resonance) of the high-affinity ubisemiquinone center in cytochrome *bo*$_3$ from *Escherichia coli*, *Biochemistry 39*, 3169−3175.
26. Rigby, S. E., Evans, M. C., and Heathcote, P. (1996) ENDOR and special triple resonance spectroscopy of A_1^- of photosystem 1, *Biochemistry 35*, 6651−6656.
27. MacMillan, F., Lendzian, F., Renger, G., and Lubitz, W. (1995) EPR and ENDOR investigation of the primary electron acceptor radical anion Q_A^- in iron-depleted photosystem II membrane fragments, *Biochemistry 34*, 8144−8156.
28. Salerno, J. C., Osgood, M., Liu, Y. J., Taylor, H., and Scholes, C. P. (1990) Electron nuclear double resonance (ENDOR) of the Q_c^- ubisemiquinone radical in the mitochondrial electron transport chain, *Biochemistry 29*, 6987−6993.
29. Lubitz, W., Abresch, E. C., Debus, R. J., Isaacson, R. A., Okamura, M. Y., and Feher, G. (1985) Electron nuclear double resonance of semiquinones in reaction centers of *Rhodopseudomonas sphaeroides*, *Biochim. Biophys. Acta 808*, 464−469.
30. Magalon, A., Rothery, R. A., Lemesle-Meunier, D., Frixon, C., Weiner, J. H., and Blasco, F. (1998) Inhibitor binding within the NarI subunit (cytochrome b_{nr}) of *Escherichia coli* nitrate reductase A, *J. Biol. Chem. 273*, 10851−10856.
31. Fisher, N., and Rich, P. R. (2000) A motif for quinone binding sites in respiratory and photosynthetic systems, *J. Mol. Biol. 296*, 1153−1162.
32. Hastings, S. F., Kaysser, T. M., Jiang, F., Salerno, J. C., Gennis, R. B., and Ingledew, W. J. (1998) Identification of a stable semiquinone intermediate in the purified and membrane bound ubiquinol oxidase-cytochrome *bd* from *Escherichia coli*, *Eur. J. Biochem. 255*, 317−323.
33. Maklashina, E., Hellwig, P., Rothery, R. A., Kotlyar, V., Sher, Y., Weiner, J. H., and Cecchini, G. (2006) Differences in protonation of ubiquinone and menaquinone in fumarate reductase from *Escherichia coli*, *J. Biol. Chem. 281*, 26655−26664.
34. Hagerhall, C., Magnitsky, S., Sled, V. D., Schroder, I., Gunsalus, R. P., Cecchini, G., and Ohnishi, T. (1999) An *Escherichia coli* mutant quinol:fumarate reductase contains an EPR-detectable semiquinone stabilized at the proximal quinone-binding site, *J. Biol. Chem. 274*, 26157−26164.
35. Iverson, T. M., Luna-Chavez, C., Croal, L. R., Cecchini, G., and Rees, D. C. (2002) Crystallographic studies of the *Escherichia coli* quinol-fumarate reductase with inhibitors bound to the quinol-binding site, *J. Biol. Chem. 277*, 16124−16130.
36. Mogi, T., Akimoto, S., Endou, S., Watanabe-Nakayama, T., Mizuochi-Asai, E., and Miyoshi, H. (2006) Probing the ubiquinol-binding site in cytochrome *bd* by site-directed mutagenesis, *Biochemistry 45*, 7924−7930.
37. Rodrigues, M. L., Oliveira, T. F., Pereira, I. A., and Archer, M. (2006) X-ray structure of the membrane-bound cytochrome *c* quinol dehydrogenase NrfH reveals novel haem coordination, *EMBO J. 25*, 5951−5960.
38. Kolling, D. R., Samoilova, R. I., Holland, J. T., Berry, E. A., Dikanov, S. A., and Crofts, A. R. (2003) Exploration of ligands to the Q_i site semiquinone in the *bc*$_1$ complex using high-resolution EPR, *J. Biol. Chem. 278*, 39747−39754.
39. Flores, M., Isaacson, R., Abresch, E., Calvo, R., Lubitz, W., and Feher, G. (2007) Protein-cofactor interactions in bacterial reaction centers from *Rhodobacter sphaeroides* R-26: II. Geometry of the hydrogen bonds to the primary quinone formula by 1H and 2H ENDOR spectroscopy, *Biophys. J. 92*, 671−682.
40. Zhao, Z., Rothery, R. A., and Weiner, J. H. (2003) Transient kinetic studies of heme reduction in *Escherichia coli* nitrate reductase A (NarGHI) by menaquinol, *Biochemistry 42*, 5403−5413.

BI700074Y